Detection of Cell Membrane Interactions with Lipid-functionalized Single-walled Carbon Nanotubes

Nathaniel Kallmyer
Iowa State University
Danielle Eeg
Iowa State University
Rachel Khor
Iowa State University
Nathan Roby
Iowa State University
Nigel Reuel (reuel@iastate.edu)
Iowa State University https://orcid.org/0000-0003-3438-2919

Article

Keywords: membranes, drug delivery, antimicrobials applications

Posted Date: June 11th, 2021

DOI: https://doi.org/10.21203/rs.3.rs-588765/v1

Abstract

Membrane-active molecules are of great importance to drug delivery and antimicrobials applications. While the ability to prototype new membrane-active molecules has improved greatly with the advent of automated chemistries and rapid biomolecule expression techniques, testing methods are still limited by throughput, cost, and modularity. Existing methods suffer from feasibility constraints of working with pathogenic, living cells and by intrinsic limitations of model systems. Herein, we demonstrate an abiotic sensor that uses semiconducting single-walled carbon nanotubes (SWNT) as near infrared fluorescent transducers to report membrane interactions. This sensor is comprised of SWNT aqueously suspended in a phospholipid monolayer; these SWNT probes are very sensitive to solvent access (changes in permittivity) and thus report morphological changes to the membrane by modulation of fluorescent signal where binding and disruption are reported as brightening and attenuation, respectively. This mechanism is first demonstrated with chemical and physical membrane-disruptive agents including ethanol, sodium dodecyl sulfate, and application of electrical pulses. Known cell-penetrating and antimicrobial peptides are then used to demonstrate how the dynamic response of these sensors can be deconvoluted to evaluate different, parallel mechanisms of interaction. Lastly, SWNT functionalized in several different bacterial lipopolysaccharides (*P aeruginosa*, *K pneumoniae*, and *E coli*) are used to evaluate a panel of known membrane-disrupting antimicrobials to demonstrate that drug selectivity can be assessed by suspension of SWNT with different membrane materials.

Introduction

The cellular membrane is a key obstacle to a variety of biological applications spanning drug delivery, cell transformation, and antimicrobials development. Developing molecules to penetrate or disrupt the membrane is a frequent goal in various screening campaigns. These campaigns involve iterative prototyping and testing various molecules to discover and optimize new candidates. While the ability to produce new membrane-interacting molecules has improved vastly with the improvement and development of protein-expression techniques[1–3], testing remains a bottleneck.

Existing methods to screen membrane interactions vary from direct assays with target cells to assays with model systems such as liposomes, planar membranes, or monolayers (summarized in Table 1). While the most accurate model for testing is the target cell, living cells require maintenance and may behave stochastically. Furthermore, discovery campaigns with live cells require stringent biological containment protocols and engineered barriers both to prevent exposure of cells to contaminants and to prevent exposure of researchers to infectious material. Cell assays also suffer limitations specific to the application. Fluorescent microscopy assays, common for drug delivery applications, can be used to straightforwardly determine an uptake efficiency but require imaging analysis that is not easily adapted for automated, high-throughput processes. Growth inhibition and cell death assays (common for antimicrobials development) are subject to timescales of cell growth, often overnight if not multiple day processes. These long response times can further introduce inconsistencies. Depending on the duration, antimicrobial depletion and bacterial regrowth can further contribute to variability[4]. Mechanistic

information is also limited, as observations often only describe end effects. While reporter cell lines do exist and enable mechanism-specific tests (often reported by expression of differently colored fluorescent proteins)[5,6], these are constrained to specific mechanisms on model cultures. Thus, while target cell tests are a necessary step in drug development, they are not necessarily an effective screening tool for lead discovery and optimization.

Abiotic model systems use membranes as proxies to avoid problems related to living cells. Synthetic liposomes containing various transduction elements may be easily prepared for leakage tests; however, they have limited temporal resolution and often only indicate activity towards a generalized membrane. Surface plasmon resonance (SPR) reports interactions on a membrane surface in real time, providing information useful for prediction of mechanisms, but requires regeneration of the surface for successive tests, a step which can be a lengthy depending on reverse kinetics (assuming the measured interaction is reversible). Thus, SPR is an effective diagnostic tool but lacks the throughput necessary for larger screening applications.

Table 1. Common experimental techniques for measuring membrane interactions

Assay	Description	Advantages	Limitations
Target cell assays[4]	Directly evaluate function on target cell by fluorescent labelling, cell death assays, or growth inhibition tests	High applicability of data; Necessary step in translational work; Inexpensive	Difficult to evaluate mechanism; Subject to safety constraints of target cells; Limited by timescale of cell growth; Possibility for regrowth; Cells require maintenance
Evanescent field sensing (SPR, PWR, OWLS, DPI, etc)[7]	Measure changes to membrane structure within evanescent field based on optical phase difference measurements	Real-time measurements; Sometimes abiotic; Automatable	Membrane regeneration times; Solid-state sensor complicates automation; Expensive; Difficult to multiplex for high-throughput screening
Liposome or vesicle assays[8–11]	Transduce penetration by turn-on response triggered by exposure of probe to liposome contents	Potentially high throughput; Abiotic; Highly compatible with combinatorial screening strategies; Automatable	Limited effectiveness for asymmetric membranes; Difficult to implement with non-amide drug candidates; Form factor limits measured interactions
Nuclear magnetic resonance/electron spin resonance[12,13]	Attach labels to membrane and determine structure based on peak splitting	High selectivity; Effective complementary technique	Requires expensive labels; Generally low throughput
Direct structural characterization (AFM, EM)[14–16]	Direct imaging of membrane surface in search for aberrations	Direct visualization of mechanisms; Effective complementary technique	Very low throughput, Lack of time resolution; High capital cost; Technically challenging

Semiconducting single-walled carbon nanotubes (SWNT) are near infrared fluorescent transducers that offer sensitivity similar to SPR. SWNT are uniquely sensitivity to their local dielectric environment which enables transduction of various phenomena by modulation of fluorescent signal[17]. For use in aqueous environments, SWNT must be noncovalently functionalized by suspension in an amphiphilic polymer or surfactant. This functionalization produces a corona phase around the nanotube which ultimately determines interactions between the resulting sensor and its environment[18]. The combined surface sensitivity and modular method of functionalization result in a powerful sensing platform where transduction may occur without the conventional energy donor-acceptor pair (e.g., tethered FRET pair or quenching agent). While much established work has been applied to sensing binding events[18–20], recent studies have demonstrated SWNT's ability to transduce direct modification to the corona phase[21,22]. This manuscript represents a shift from sensing chemical modifications to the corona phase (e.g., hydrolytic enzyme modification) to detecting structural changes (e.g., pore formation and disruption). By exploiting

the strong quenching effect of water[23], these sensors could be used to detect morphological changes to the corona phase. Thus, if functionalized in membrane lipids, SWNT should be able to transduce structural changes to this monolayer.

In this work, we demonstrate that SWNT sensors can report membrane interactions in real time while retaining the adaptability of a solution-phase fluorescent sensor. As proof of concept, we first demonstrate that, when functionalized with phosphatidylcholine (PC) or lipopolysaccharides (LPS), SWNT respond to membrane disruption by fluorescence quenching. We then test these sensors against different concentrations of membrane-active peptides and show several distinct kinetic and dynamic behaviors corresponding to different mechanisms. Lastly, we screen SWNT functionalized with several different LPS against a panel of potential membrane-active antimicrobials at different concentrations to demonstrate the potential selectivity and throughput of this technique.

Results

In this study, SWNT were suspended in PC or LPS to produce sensors with surface functionality similar to outer cell membranes. These sensors, now cloaked by a hemimicelle, transduce membrane binding and disruption events as modulation of fluorescence intensity (Fig 1). This modulation likely results from changes to accessibility of the SWNT surface to water, which behaves as a quenching agent[23]. Therefore, binding and further cladding of the hemimicelle would cause brightening, while disruption, whether a result of binding, translocation, or pore formation, would cause quenching.

Sensor Preparation

Prior to testing sensors, the suspension process for PC-SWNT was optimized based on a central composite designed experiment (more details in Supplement 1), as initial attempts to suspend PC-SWNT yielded sensors which failed to fluoresce significantly above background, and sonication parameters had been demonstrated in a prior study to strongly influence starting signal intensity[24]. Optimal preparation conditions were achieved with maximum lipid concentration (20 mg/mL), maximum sonication time (80 min), and minimum sonication power (2 W). It is important to note that, because signal intensity was measured after diluting sensors to a single concentration (5 mg/mL), this optimum lipid concentration was an effect of the sonication process and not the concentration-dependent hemimicelle stability. In contrast, LPS-SWNT suspended easily at a lower lipid concentration (2.5 mg/mL), likely due to a greater avidity of the larger molecule to the SWNT surface.

Membrane Disruption

SWNT sensors were first tested by orthogonal methods of membrane disruption. First, SWNT functionalized with PC were exposed to representative membrane-disrupting agents, ethanol (a chaotropic agent), and sodium dodecyl sulfate (SDS), a competing surfactant. Both of these agents caused significant quenching effects (Fig 2a,b). Sensor responses were notably fast, as fluorescent signal had already stabilized in the time required to uncover the fluorimeter, add sample, and re-cover the

fluorimeter. SWNT functionalized with LPS from *E coli* serotype O127 were tested in electroporation conditions by connecting a custom sample holder to a piezoelectric igniter (Supplement 2), a setup based on the inexpensive ElectroPen[25], and applying pulses every 60 s (Fig 2c). These pulses caused quenching events lasting 3-4 s before recovery of signal (dynamics shown in Supplement 2). Changes in signal observed after recovery are associated with jostling of the sample holder rather than irreversible changes to the sensors.

Sensor Response Dynamics

PC- and LPS-SWNT were then tested against membrane-active peptides to observe response dynamics. First, sensors were tested with TAT peptide, a cationic peptide derived from a transcription factor of HIV, notable for its efficacy in mediating cellular delivery[26]. Addition of TAT peptide caused rapid quenching to both PC-SWNT and LPS-SWNT (Fig 3a,b). This quenching was most pronounced with the more negatively charged LPS. The fast rate of quenching suggests a disruption mechanism that occurred immediately upon binding. Two dynamic behaviors were observed around concentration thresholds (Fig 3b,c). At low concentrations, fluorescent signal increased with respect to peptide concentration, indicating non-disruptive binding. Above this threshold, rapid quenching was observed. This threshold likely represents a critical concentration above which surface coverage is sufficient to achieve a disruption event. The rate and dynamic behavior of these responses are consistent with the carpet model, in which the cationic peptides coat or “carpet” the membrane surface and disrupt the packing structure of lipids before ultimately behaving as detergents at higher concentrations[27].

PC- and LPS-SWNT were also exposed to an amphipathic peptide derived from crotamine, a protein in South American rattlesnake venom[28]. In contrast to the fast responses from TAT peptide, this amphipathic peptide elicited a gradual quenching response, spanning minutes, from both PC-SWNT and LPS-SWNT (Fig 4a,b). This would suggest a separate mechanism from that observed with the TAT peptide. The PC- and LPS-SWNT both featured a threshold-based dynamic behavior similar to that observed with the TAT peptide (Fig 4c,d); however, as concentration increased further beyond the observed threshold, the quenching effect diminished. This recovery of signal may be associated with the amphiphilic nature of the peptide and the lability of the original lipid-surfactant hemimicelle. At such a concentration, the peptide would begin to displace the lipids, forming a new corona phase.

Screening Tools for Antimicrobials

To evaluate selectivity of these sensors and validate their performance, SWNT functionalized with LPS from *Pseudomonas aeruginosa*, *Klebsiella pneumoniae*, and *E coli* (serotype O26) were tested against a panel of different membrane-disrupting antibiotics (Fig 6). These antimicrobials were tested at different concentrations to evaluate concentration dynamics, and distinct response components were evaluated to determine any variations of apparent interaction mechanism. Relative to the other LPS-SWNT, *K pneumoniae* SWNT produced little fluorescent signal, only slightly above background. This may explain the relatively small signal changes seen from this sensor. If LPS from *K pneumoniae* only weakly

protected the nanotube surface from water, producing a sensor with low starting fluorescence, any disruptions to this hemimicelle would be less apparent and would produce smaller relative signal changes. SWNT functionalized with *E coli* LPS yielded strong quenching effects with most antimicrobials. The broad selectivity suggests high susceptibility to disruption by detergents. Additionally, *E coli* SWNT demonstrated significantly slower responses than the other sensors, particularly to colistin. This slowed response behavior was seen previously with the crotamine-derived peptide and, again, suggests that response dynamics vary with lipid. Both slowed responses occurring with different *E coli* SWNT also suggests that the LPS component responsible for this behavior is conserved. The lipid A moiety would fit this criterion, as it is both highly conserved within species and would strongly govern the mode of LPS-SWNT interaction.

Of the tested antimicrobials, colistin's effects were most apparent, with strong quenching effects at all concentrations for *P aeruginosa* LPS-SWNT and quenching starting at 20 μM and 5 μM for *K pneumoniae* and *E coli* LPS-SWNT, respectively. This distinctly high activity against *P aeruginosa* was expected, as MICs of colistin against non-colistin-resistant *P aeruginosa* fall within a range approximately an order of magnitude lower than those for *K pneumoniae* and *E coli*. Additionally, these thresholds occurred at concentrations comparable to MICs reported in literature (0.069 – 18.5 μM for *P aeruginosa*, 0.29 – 148 μM for *K pneumoniae*, and 0.14 – 148 μM for *E coli*)[29–31]. With the exception of *E coli* SWNT, which produced relatively slow responses, colistin's effects were primarily seen in an initial, fast-kinetics quenching event. Interestingly, following this quenching, a gradual brightening effect was observed which diminished with increasing concentration. This brightening was likely an effect of reorientation of colistin-bound lipids following the initial disruptive shock. This mechanism would also explain the diminishing brightening effect with increased concentration, as increased multivalent binding by colistin would hinder reorientation of lipids.

In contrast to colistin, G10KHc, a peptide designed to selectively bind and kill *Pseudomonas* bacteria[32], failed to cause quenching to the *P aeruginosa* SWNT and only caused quenching effects at high concentrations for *K pneumoniae* and *E coli*. This lack of selectivity towards *P aeruginosa* probes may the result of a protein (e.g., a porin) binding target rather than the LPS itself. LPS-SWNT would lack these features and, thus, would be incapable of transducing this bactericidal mechanism. This highlights a limitation of these SWNT sensors, an inability to reproduce protein-dependent mechanisms.

For *P aeruginosa* and *K pneumoniae*, triton X-100's activity was seen in a fast-kinetics response. While most apparent with *P aeruginosa* SWNT, a transition can be seen with the *K pneumoniae* SWNT as a relatively strong brightening effect diminishes. Relative to the other antimicrobials, melittin elicited little response from *P aeuruginosa* SWNT. In contrast, melittin produced a strong quenching response with *K pneumoniae* SWNT, nearly matching that observed with colistin.

Interestingly, the PC-SWNT response to the amphipathic peptide (Fig 4a) featured both fast-kinetics and slow-kinetics components, potentially indicating two mechanisms occurring in parallel. Because these apparent mechanisms occurred at significantly different rates, it was possible to deconvolute this

response by separately evaluating initial, fast-kinetics and subsequent, slow-kinetics signal changes, as shown in Figure 5a. The fast-kinetics response (Fig 5b) featured the same threshold-based dynamic behavior seen in the total response. The later, slow-kinetics response (Fig 5c), however, changed continuously with concentration. While non-linear with respect to bulk peptide concentration (Fig 5d), the responses were strongly linear when fit to a Langmuir isotherm (Fig 5e), suggesting that this slow-kinetics response occurred distinctly after adsorption and with first-order kinetics. This was consistent with diffusion of peptide through the hemimicelle, as diffused peptides would accumulate within the hemimicelle and cause signal-quenching deformities. Although relative timescales would suggest that the slow-kinetics responses from *E coli* LPS-SWNT were also the result of translocation, the threshold-based dynamic behavior (Fig 4d) suggests a disruptive mechanism similar to that seen in the fast-kinetics responses. This would indicate that, while mechanisms may be temporally deconvoluted, interpretation of this data must be performed on an individual sensor basis.

Screening Tools for Antimicrobials

To evaluate selectivity of these sensors and validate their performance, SWNT functionalized with LPS from *Pseudomonas aeruginosa*, *Klebsiella pneumoniae*, and *E coli* (serotype O26) were tested against a panel of different membrane-disrupting antibiotics (Fig 6). These antimicrobials were tested at different concentrations to evaluate concentration dynamics, and distinct response components were evaluated to determine any variations of apparent interaction mechanism. Relative to the other LPS-SWNT, *K pneumoniae* SWNT produced little fluorescent signal, only slightly above background. This may explain the relatively small signal changes seen from this sensor. If LPS from *K pneumoniae* only weakly protected the nanotube surface from water, producing a sensor with low starting fluorescence, any disruptions to this hemimicelle would be less apparent and would produce smaller relative signal changes. SWNT functionalized with *E coli* LPS yielded strong quenching effects with most antimicrobials. The broad selectivity suggests high susceptibility to disruption by detergents. Additionally, *E coli* SWNT demonstrated significantly slower responses than the other sensors, particularly to colistin. This slowed response behavior was seen previously with the crotamine-derived peptide and, again, suggests that response dynamics vary with lipid. Both slowed responses occurring with different *E coli* SWNT also suggests that the LPS component responsible for this behavior is conserved. The lipid A moiety would fit this criterion, as it is both highly conserved within species and would strongly govern the mode of LPS-SWNT interaction.

Of the tested antimicrobials, colistin's effects were most apparent, with strong quenching effects at all concentrations for *P aeruginosa* LPS-SWNT and quenching starting at 20 μM and 5 μM for *K pneumoniae* and *E coli* LPS-SWNT, respectively. This distinctly high activity against *P aeruginosa* was expected, as MICs of colistin against non-colistin-resistant *P aeruginosa* fall within a range approximately an order of magnitude lower than those for *K pneumoniae* and *E coli*. Additionally, these thresholds occurred at concentrations comparable to MICs reported in literature (0.069 – 18.5 μM for *P aeruginosa*, 0.29 – 148 μM for *K pneumoniae*, and 0.14 – 148 μM for *E coli*)[29–31]. With the exception of *E coli* SWNT, which produced relatively slow responses, colistin's effects were primarily seen in an initial, fast-kinetics

quenching event. Interestingly, following this quenching, a gradual brightening effect was observed which diminished with increasing concentration. This brightening was likely an effect of reorientation of colistin-bound lipids following the initial disruptive shock. This mechanism would also explain the diminishing brightening effect with increased concentration, as increased multivalent binding by colistin would hinder reorientation of lipids.

In contrast to colistin, G10KHc, a peptide designed to selectively bind and kill *Pseudomonas* bacteria[32], failed to cause quenching to the *P aeruginosa* SWNT and only caused quenching effects at high concentrations for *K pneumoniae* and *E coli*. This lack of selectivity towards *P aeruginosa* probes may the result of a protein (e.g., a porin) binding target rather than the LPS itself. LPS-SWNT would lack these features and, thus, would be incapable of transducing this bactericidal mechanism. This highlights a limitation of these SWNT sensors, an inability to reproduce protein-dependent mechanisms.

For *P aeruginosa* and *K pneumoniae*, triton X-100's activity was seen in a fast-kinetics response. While most apparent with *P aeruginosa* SWNT, a transition can be seen with the *K pneumoniae* SWNT as a relatively strong brightening effect diminishes. Relative to the other antimicrobials, melittin elicited little response from *P aeuruginosa* SWNT. In contrast, melittin produced a strong quenching response with *K pneumoniae* SWNT, nearly matching that observed with colistin.

Discussion

Herein, we have demonstrated that SWNT functionalized with membrane materials, such as phosphatidylcholine or lipopolysaccharides, can be used as sensors to evaluate morphological changes to a corresponding membrane surface. Because these changes occur in the immediately proximity to the transducer, this sensor has fast response times, reporting effects at timescales of seconds to minutes. Additionally, this solution-phase sensor can be easily adapted to titer-plate assays, making it suitable for high-throughput screening operations. The facile means of sensor preparation, compatibility with a ubiquitous form factor, and the accessibility of open source near infrared fluorimetry tools[22] makes this method easily adaptable for use by other laboratories.

A distinct advantage of this sensor is the ability to take measurements in real time. Within this work, we have demonstrated that sensor response traces may be deconvoluted to evaluate multiple mechanisms in parallel. Given the multitude of potential mechanisms (e.g., binding, carpet binding, toroidal pore formation, barrel pore formation), the ability to determine both magnitude and quality of interaction would be valuable for both characterization and optimization of lead molecules. While, in this work, we demonstrated a binary mode of categorization, a faster scan rate and further kinetic characterization may enable more specific categorization. With more mechanistic information, it may be possible to use these different response components to distinguish between lytic and non-lytic mechanisms and better inform the design and optimization of new cell surface targeting markers, membrane penetrating peptides, and membrane disrupting therapies.

Methods

Optimization of PC-SWNT Fluorescence

2 mL samples of PC-SWNT were suspended by probe tip sonication (Qsonica Q125, 1/8” probe) in 5 mL centrifuge tubes while cooled in an ice bath. SWNT (Chasm Advanced Materials, SG65i) were added to PC (Sigma P3556) in DI water, and this mixture of lipid solution and undissolved SWNT was then sonicated. SWNT concentration was kept at a constant 0.5 mg/mL. PC-SWNT were suspended with different combinations of PC concentration (5, 10, or 20 mg/mL in deionized water), sonication power (2, 10, or 18 W), and sonication time (40, 60, and 80 min), described in Supplement 1. Sensors were then collected as supernatant after centrifugation at 10,000 xg for 10 min. Each sensor solution was then diluted in deionized water to achieve a final PC concentration of 5 mg/mL. Fluorescent signal from each of these samples was then measured with a custom fluorimeter adapted from prior work[21]. These signal intensities were then fit to a quadratic model with respect to sonication power, sonication time, and logarithm of concentration.

Suspension of SWNT Sensors

PC-SWNT were prepared based on the previously observed optimal conditions. A 2-mL mixture with 0.5 mg/mL SWNT and 20 mg/mL PC was sonicated for 80 min at 2 W, and sensors were collected as the supernatant following centrifugation at 10,000 xg for 10 min. LPS-SWNT were suspended with different conditions. 0.5 mg/mL SWNT were suspended in 2.5 mg/mL LPS solutions by probe tip sonication at 2 W for 60 min. Sensors were similarly collected by centrifugation and collection of supernatant.

Membrane Disruption Tests

Further tests were performed on a custom near-infrared plate reader (described in a previous work)[22]. Initial disruption tests were performed with PC-SWNT diluted to a concentration of 2.5 mg/mL PC. Tests with ethanol and SDS were performed by first adding 80 µL sensor solution to wells in a 96-well plate. A fluorescent scan was then initiated and, following collection of a baseline signal, 20 µL of disruptive agent (100 mg/mL SDS or pure ethanol) were added. Electrical disruption was performed on LPS-SWNT (LPS from *E coli* serotype O127, Sigma L3129), diluted to a concentration of 0.5 mg/mL LPS, using a custom acrylic plastic sample holder which featured a 5-mm wide channel lined on two ends with copper tape. These two leads were soldered to a piezoelectric ignition element which, when triggered, would apply an electrical impulse. LPS-SWNT were added to this channel and scanned for 10 min. Starting at 60 s, the igniter was triggered every 60 s until the end of the scan. These electrical shock scans were performed in a single-scan mode.

Cell-penetrating Peptide Tests

To evaluate dynamic effect of cell-penetrating peptides on sensors, PC-SWNT and LPS-SWNT were tested with a panel of different peptide concentrations. A cationic tat-derived peptide, RKKRRQRRR (Genscript),

and an amphiphilic crotamine-derived peptide, YKQCHKKGGKKGSG (Genscript), were used to test these sensors. To determine an order of magnitude of dynamic range, initial tests were performed, as described previously (80 µL sensor, 20 µL disruptor) by serially diluting peptide samples by factors of 10, starting at 2.5 mg/mL peptide. The concentration range for further testing was then determined based on an observed quenching threshold. These further tests were then performed by serially diluted peptide solutions by factors of 2. Reported concentrations of disruptors indicate final concentrations following mixing with sensor solutions, one fifth of the concentration of peptide prior to addition.

Antimicrobial Screening

SWNT were functionalized in LPS from *Escherichia coli* (serotype O26, Sigma L8274), *Pseudomonas aeruginosa* (serotype 10, Sigma L9143), and *Klebsiella pneumoniae* (Sigma L4268) by the same procedure used previously for LPS-SWNT. LPS-SWNT were tested against a panel of potential membrane-disrupting antimicrobials that included colistin sulfate (Sigma C4461), a *Pseudomonas*-targeting peptide (KKHRKHRKHRKHGGSGGSKNLRRIIRKGIHIIKKYG, Genscript), Triton X-100 (Sigma X100), and melittin (Sigma M2272). Responses were collected by performing 20-minute scans and adding disruptors to sensors 2 minutes after beginning the scan. For *E coli* SWNT, a 20-minute, blank scan was performed prior to testing to stabilize signal.

Declarations

Acknowledgements

NEK was funded in part by USDA AFRI grant #2019-67011-29517. NFR and this project was also supported by NIH NIGMS MIRA ESI grant #1R35GM138265-01.

References

1. Mijalis, A. J. *et al.* A fully automated flow-based approach for accelerated peptide synthesis. *Nat. Chem. Biol.* **13**, 464–466 (2017).

2. Zheng, H. *et al.* An automated Teflon microfluidic peptide synthesizer. *Lab Chip* **13**, 3347–3350 (2013).

3. Dopp, J. L., Rothstein, S. M., Mansell, T. J. & Reuel, N. F. Rapid prototyping of proteins: Mail order gene fragments to assayable proteins within 24 hours. *Biotechnol. Bioeng.* **116**, 667–676 (2019).

4. Rudilla, H. *et al.* New and old tools to evaluate new antimicrobial peptides. *AIMS Microbiol.* **4**, 522 (2018).

5. Osterman, I. A. *et al.* Sorting out antibiotics' mechanisms of action: A double fluorescent protein reporter for high-throughput screening of ribosome and DNA biosynthesis inhibitors. *Antimicrob. Agents Chemother.* **60**, 7481–7489 (2016).

6. Hendriks, G. *et al.* The ToxTracker assay: novel GFP reporter systems that provide mechanistic insight into the genotoxic properties of chemicals. *Toxicol. Sci.* **125**, 285–298 (2012).

7. Lee, T.-H., Hirst, D. J. & Aguilar, M.-I. New insights into the molecular mechanisms of biomembrane structural changes and interactions by optical biosensor technology. *Biochim. Biophys. Acta (BBA)-Biomembranes* **1848**, 1868–1885 (2015).

8. Gee, M. L. *et al.* Imaging the action of antimicrobial peptides on living bacterial cells. *Sci. Rep.* **3**, 1–6 (2013).

9. Carney, R. P. *et al.* Combinatorial library screening with liposomes for discovery of membrane active peptides. *ACS Comb. Sci.* **19**, 299–307 (2017).

10. Marks, J. R., Placone, J., Hristova, K. & Wimley, W. C. Spontaneous membrane-translocating peptides by orthogonal high-throughput screening. *J. Am. Chem. Soc.* **133**, 8995–9004 (2011).

11. Zepik, H. H., Walde, P., Kostoryz, E. L., Code, J. & Yourtee, D. M. Lipid vesicles as membrane models for toxicological assessment of xenobiotics. *Crit. Rev. Toxicol.* **38**, 1–11 (2008).

12. Strandberg, E. & Ulrich, A. S. NMR methods for studying membrane-active antimicrobial peptides. *Concepts Magn. Reson. Part A An Educ. J.* **23**, 89–120 (2004).

13. Smirnova, T. I. & Smirnov, A. I. Peptide–membrane interactions by spin-labeling EPR. *Methods Enzymol.* **564**, 219–258 (2015).

14. Avci, F. G., Sariyar Akbulut, B. & Ozkirimli, E. Membrane active peptides and their biophysical characterization. *Biomolecules* **8**, 77 (2018).

15. Mio, K. & Sato, C. Lipid environment of membrane proteins in cryo-EM based structural analysis. *Biophys. Rev.* **10**, 307–316 (2018).

16. Hammond, K., Ryadnov, M. G. & Hoogenboom, B. W. Atomic force microscopy to elucidate how peptides disrupt membranes. *Biochim. Biophys. Acta (BBA)-Biomembranes* 183447 (2020).

17. Kruss, S. *et al.* Carbon nanotubes as optical biomedical sensors. *Adv. Drug Deliv. Rev.* **65**, 1933–1950 (2013).

18. Zhang, J. *et al.* Molecular recognition using corona phase complexes made of synthetic polymers adsorbed on carbon nanotubes. *Nat. Nanotechnol.* **8**, 959–968 (2013).

19. Landry, M. P. *et al.* Single-molecule detection of protein efflux from microorganisms using fluorescent single-walled carbon nanotube sensor arrays. *Nat. Nanotechnol.* **23**, (2017).

20. Salem, D. P. *et al.* Chirality dependent corona phase molecular recognition of DNA-wrapped carbon nanotubes. *Carbon N. Y.* **97**, 147–153 (2016).

21. Kallmyer, N. E., Musielewicz, J., Sutter, J. & Reuel, N. F. N. F. Substrate-Wrapped, Single-Walled Carbon Nanotube Probes for Hydrolytic Enzyme Characterization. *Anal. Chem.* **90**, 5209–5216 (2018).

22. Kallmyer, N. E. *et al.* Inexpensive Near-Infrared Fluorimeters: Enabling Translation of nIR-Based Assays to the Field. *Anal. Chem.* (2021).

23. Hertel, T. *et al.* Spectroscopy of single- and double-wall carbon nanotubes in different environments. *Nano Lett.* **5**, 511–514 (2005).

24. Kallmyer, N. E. N. *et al.* Influence of sonication conditions and wrapping type on yield and fluorescent quality of noncovalently functionalized single-walled carbon nanotubes. *Carbon N. Y.* **139**, 609–613 (2018).

25. Byagathvalli, G. *et al.* ElectroPen: An ultra-low–cost, electricity-free, portable electroporator. *PLoS Biol.* **18**, e3000589 (2020).

26. Brooks, H., Lebleu, B. & Vivès, E. Tat peptide-mediated cellular delivery: back to basics. *Adv. Drug Deliv. Rev.* **57**, 559–577 (2005).

27. Yeaman, M. R. & Yount, N. Y. Mechanisms of antimicrobial peptide action and resistance. *Pharmacol. Rev.* **55**, 27–55 (2003).

28. Rádis-Baptista, G., de la Torre, B. G. & Andreu, D. Insights into the uptake mechanism of NrTP, a cell-penetrating peptide preferentially targeting the nucleolus of tumour cells. *Chem. Biol. Drug Des.* **79**, 907–915 (2012).

29. Walkty, A. *et al.* In vitro activity of ceftazidime combined with NXL104 versus Pseudomonas aeruginosa isolates obtained from patients in Canadian hospitals (CANWARD 2009 study). *Antimicrob. Agents Chemother.* **55**, 2992–2994 (2011).

30. Yau, Y. H., Ho, B., Tan, N. S., Ng, M. L. & Ding, J. L. High therapeutic index of factor C Sushi peptides: potent antimicrobials against Pseudomonas aeruginosa. *Antimicrob. Agents Chemother.* **45**, 2820–2825 (2001).

31. Souli, M. *et al.* In vitro activity of tigecycline against multiple-drug-resistant, including pan-resistant, gram-negative and gram-positive clinical isolates from Greek hospitals. *Antimicrob. Agents Chemother.* **50**, 3166–3169 (2006).

32. Eckert, R. *et al.* Adding selectivity to antimicrobial peptides: Rational design of a multidomain peptide against Pseudomonas spp. *Antimicrob. Agents Chemother.* **50**, 1480–1488 (2006).

Figures

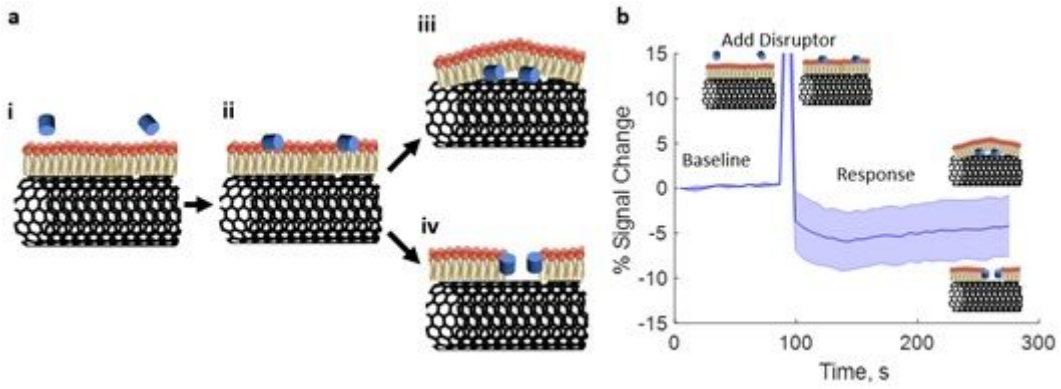

Figure 1

(a) Scheme of transduction mechanism. Membrane functionalized SWNT (i) are exposed to membrane-interacting molecules which can then (ii) bind to the surface of the membrane and subsequently (iii) diffuse through the membrane or (iv) self-assemble and form pores. (b) Sample sensor response (shaded region indicates one standard deviation, n = 4). Spike in signal seen during addition of disruptor occurs when the fluorimeter is uncovered and exposed to ambient light.

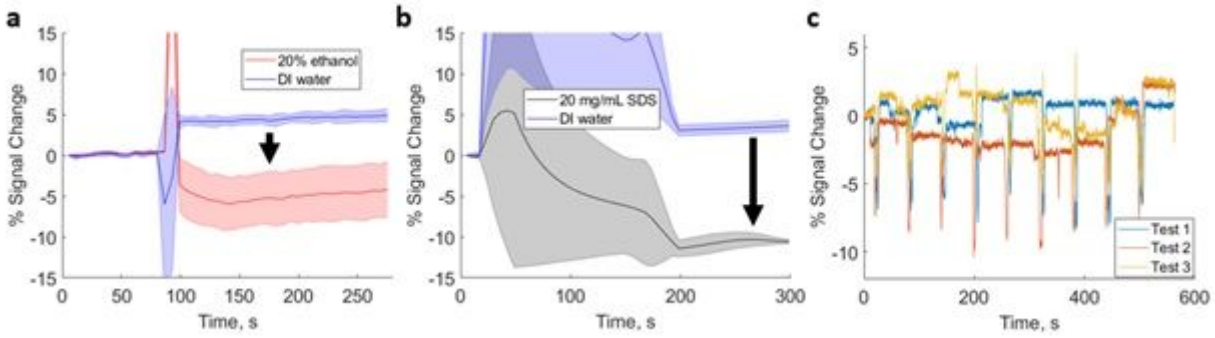

Figure 2

(a) Temporal response of PC-SWNT to addition of ethanol. (b) Temporal response of phosphatidylcholine-SWNT to addition of sodium dodecyl sulfate. Shaded regions in (a) and (b) indicate a single standard deviation (n = 4). Periods of elevated signal at middle of scans indicate time at which disrupting agents were added. (c) Temporal response of LPS (E. coli serotype O127)-SWNT to electrical fields, applied every 60 s.

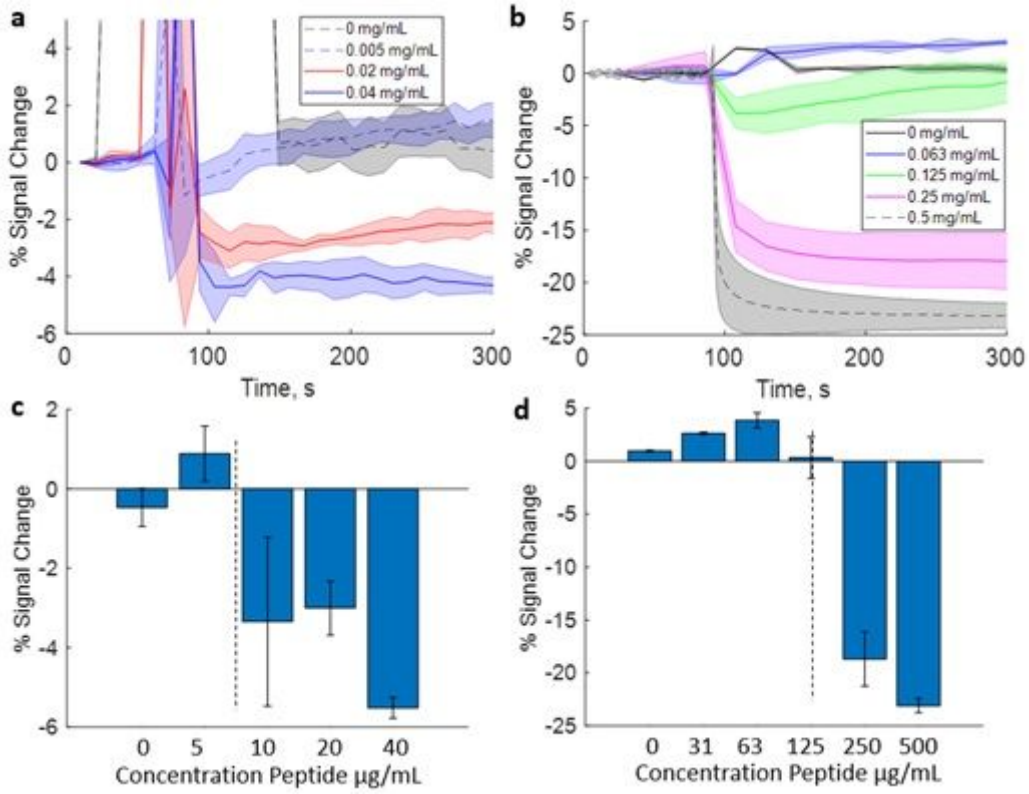

Figure 3

Temporal sensor responses of (a) phosphatidylcholine-SWNT and (b) LPS-SWNT to the TAT peptide. Shaded regions indicate a single standard deviation (n = 4). Final signal changes observed at different concentrations of TAT peptide for (c) phosphatidylcholine-SWNT and (d) LPS-SWNT. Error bars indicate a single standard deviation (n = 4). Dashed lines approximate threshold between binding and disruption regimes.

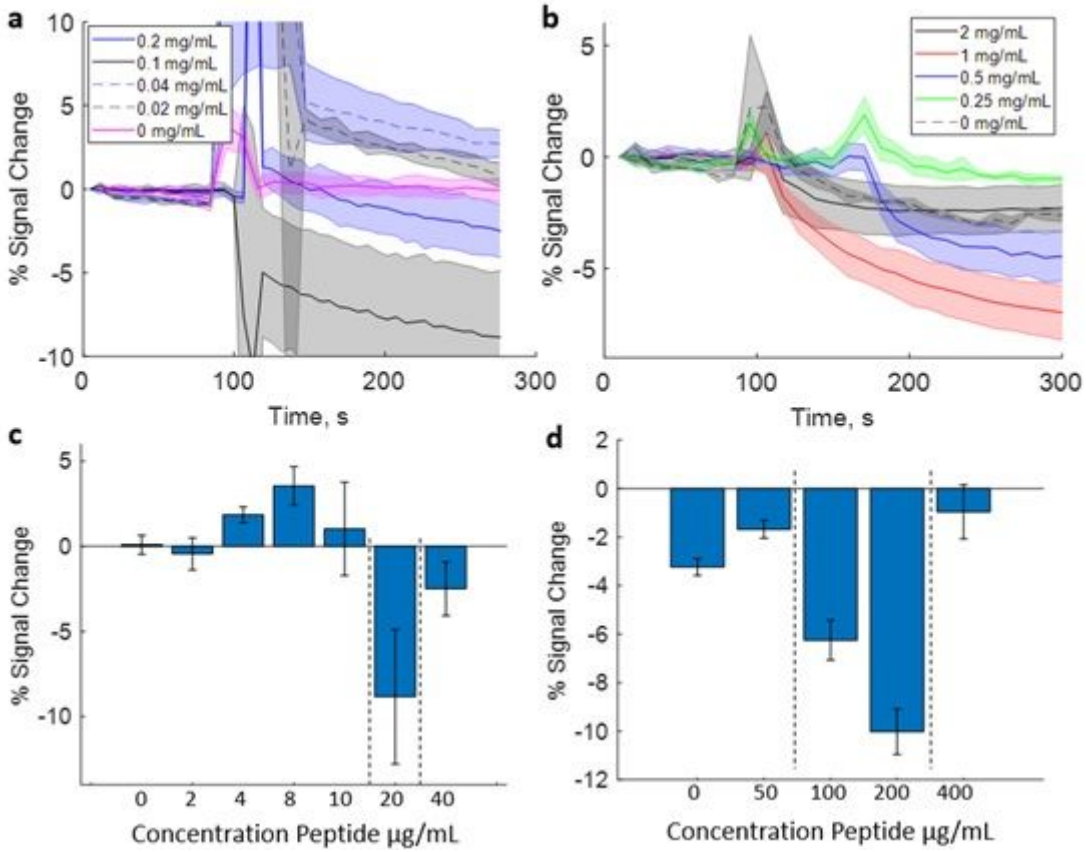

Figure 4

Temporal sensor responses of (a) phosphatidylcholine-SWNT and (b) LPS-SWNT to the crotamine-derived amphipathic peptide. Shaded regions indicate a single standard deviation (n = 4). Final signal changes observed at different concentrations of amphipathic peptide for (c) phosphatidylcholine-SWNT and (d) LPS-SWNT. Error bars indicate a single standard deviation (n = 4). Left dashed lines approximate threshold between binding and disruption regimes. Right dashed lines indicate a second transition from disruption to displacement.

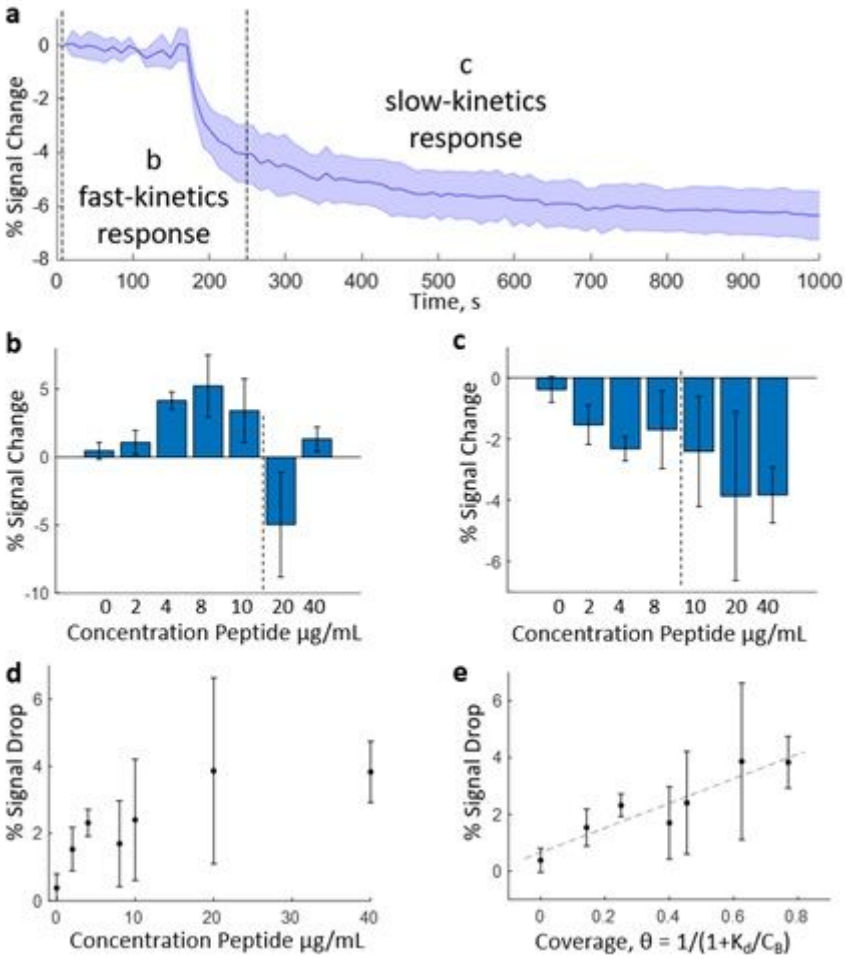

Figure 5

(a) Sample sensor response separated into different response components: (b) fast-kinetics sensor response and (c) slow-kinetics sensor response. Dashed lines indicate the apparent location of the membrane disruption concentration threshold. (d) Slow-kinetics sensor responses plotted against peptide concentration. (e) Slow-kinetics sensor response plotted against a Langmuir isotherm. Error bars and shaded regions indicate a single standard deviation (n = 4).

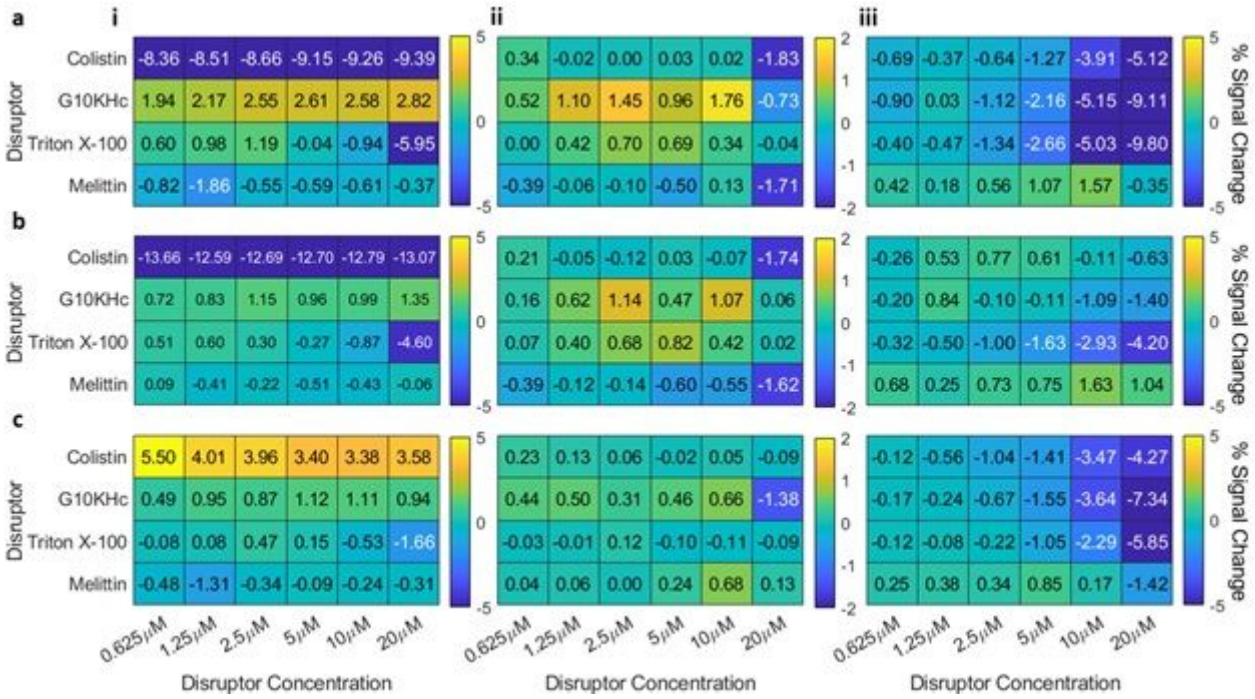

Figure 6

Heat maps indicating (a) total, (b) fast-kinetics, and (c) slow-kinetics sensor responses (% signal change) with respect to disruptor and disruptor concentrations for (i) Pseudomonas aeruginosa, (ii) Klebsiella pneumoniae, and (iii) Escherichia coli (O26) LPS-SWNT.

Supplementary Files

This is a list of supplementary files associated with this preprint. Click to download.

- Supplementv2.pdf